DETECTION OF THREE DISTINCT REGIONS IN THE EQUATORIAL ELECTROJET IN THE BRAZILIAN SECTOR

Clezio M. Denardini,[1] Mangalathayil A. Abdu,[2] José H. A. Sobral[3]

ABSTRACT

We carried out an equatorial electrojet campaign in December 1999, using the RESCO coherent backscatter radar at São Luís, at the geomagnetic equator. In this paper we selected the period from December 11 through December 19, which covers both relatively disturbed and quiet days. For this period 16 spectrograms were obtained for each day of observation with each spectrogram corresponding to one range gate. The first gate corresponds to 97.4-km height while the last gate corresponds to 115.6-km and they were sampled at 2.6-km intervals. Daily Range Time Intensity maps were generated for this period. Through the analysis of the spectrograms and considering the enhancements in the equatorial electrojet observed in the evening of some days, it was possible to observe three distinct regions as identified earlier by Pfaff and others (1987) and Kudeki and others (1987). Indeed, our observations agree with the Condor Equatorial Electrojet Campaign results. We have used the auroral activity indexes AU and AL as well as the equatorial ring current index D_{st} to evaluate the response of the equatorial electrojet to magnetic disturbances.

Keywords: 3-meter Ionospheric Irregularities, Two-Stream Instabilities, Gradient Drift Instabilities, Equatorial Electrojet, Coherent Back-scatter Radar.

RESUMO

Em dezembro de 1999 realizou-se uma campanha de coleta de dados do eletrojato equatorial, usando-se o radar de espalhamento coerente (RESCO), em São Luís, sob o equador magnético. Neste artigo, selecionamos o período de 11 a 19 de dezembro, que cobre uma etapa magneticamente calma e outra relativamente perturbada. Para este período, 16 espectrogramas foram obtidos a cada dia de observação, onde cada espectrograma corresponde a uma faixa de amostragem em altura. A primeira faixa de amostragem esta centrada em 97,4 km de altitude, enquanto a última corresponde à altura central de 115,6 km, e cada faixa possui uma extensão de 2,6 km. Mapas Diários de Variação Temporal de Intensidade foram gerados para o referido período. Pela análise dos espectrogramas e considerando a intensificação do eletrojato equatorial ao entardecer de alguns dias, foi possível observar três regiões distintas como já foi mencionado por Pfaff et al (1987) e Kudeki et al (1987). Na verdade, nossas observações concordam com os resultados da Campanha Condor de observação do eletrojato. Usamos os índices de atividade auroral AU e AL, além do índice D_{st}, relacionado à corrente anelar, para avaliar a resposta do eletrojato equatorial às perturbações magnéticas.

Palavras-chave: Irregularidades Ionosféricas de três metros, instabilidades de dois feixes, instabilidades do tipo deriva de gradiente, eletrojato equatorial, radar de espalhamento coerente.

[1] Instituto Nacional de Pesquisas Espaciais - Divisão de Aeronomia – CEA. Av. Dos Astronautas, 1758 – 12201-970, São José dos Campos, SP, Brasil – Fone: (12) 3545-7156 – Fax: (12) 3945-6990 – E-mail: denardin@dae.inpe.br.

[2] Instituto Nacional de Pesquisas Espaciais – Divisão de Aeronomia – CEA. Av. Dos Astronautas, 1758 – 12201-970, São José dos Campos, SP, Brasil – Fone: (12) 3545-7149 – Fax: (12) 3945-6990 – E-mail: maabdu@dae.inpe.br.

[3] Instituto Nacional de Pesquisas Espaciais – Divisão de Aeronomia – CEA. Av. Dos Astronautas, 1758 – 12201- 970, São José dos Campos, SP, Brasil. – Fone: (12) 3545-7147 – Fax: (12) 3945-6990 – E-mail: sobral@dae.inpe.br.

INTRODUCTION

The equatorial electrojet (EEJ) is part of a global system of electric field and currents driven by neutral wind action. It is a strong essentially horizontal eastward current (BALSLEY, 1966). It is confined along with the magnetic equator at the E region height due to the higher E regions conductivity about 95 - 115 km. It is caused by the polarization field formed by the drastic decrease in the vertical conductivity, which drives a strong additional Hall current superimposed to the previous Pedersen current caused by east-west electric fields (FORBES, 1981; REDDY, 1981; REDDY, 1989). In the presence of this current and an electron density gradient, plasma instabilities are generated. These instabilities have been intensively studied theoretically and experimentally[1]. They drive fluctuations in the local plasma density called plasma irregularities. The main characteristics of these irregularities are: (a) they are magnetic field aligned; (b) they have larger extensions along the magnetic field line than parallel to it; and (c) they have been observed during day and night, except during sunrise and sunset. We have used the RESCO coherent backscatter VHF radar at the equatorial station São Luís (2.33° S; 44.2° W; dip: -0.5 °), to investigate the behavior of the 3-m irregularities in the Brazilian sector during quiet and disturbed conditions.

THE 50 MHZ VHF RADAR SYSTEM

The RESCO 50 MHz coherent back-scatter radar was developed and constructed at INPE for the EEJ investigation and has been fully operational at São Luís - SLZ since 1999 when EEJ 3-meter plasma irregularity observations started being routinely carried out according to the International Geophysical Calendar days or some time based on emerging requirements. The basic features of the radar system details at the time the data set used in the present work was collected were:
a) Modular transmitter system consisting of 8 phase locked transmitters;
b) Attainable total peak power: 120 kW;
c) Antenna system for transmission and reception: coaxial collinear broadside array of 16 antennas, each antenna having 48 dipoles aligned in magnetic North-South; and
d) Two-way beam widths: $\sim$5° E-W plane and $\sim$2.5° N-S plane, settable in east-west plane.

In December 1999, the radar was operated to investigate the daytime EEJ 3-meter plasma irregularities using the following operational mode:
a) Peak power: $\sim$40 kW;

b) Theoretically estimated height resolution: 7.5km (oblique beam at 30° zenith angle);
c) Oblique beam tilted westward by 30° in zenith angle;
d) Inter-pulse period: 1 ms (Pulse repetition rate: 1.000Hz);
e) Pulse width: 20µs;
f) Echo sampling: 3km in range or 2.6km in height; and
g) Time resolution: 1 minute averaged.

DATA ACQUISITION AND DATA ANALYSIS

Coherent backscatter radars are sensitive to electron density fluctuation (plasma irregularities) with wavelength ($\lambda_{irregularity}$) corresponding to the radar wavelength (λ_{radar}) as:

$$\lambda_{irregularity} = \frac{\lambda_{radar}}{2\sin(\theta/2)} \ , \tag{1}$$

with θ being the angle between the wave vectors of the transmitted radar signal and the backscattered echo. In case of monostatic radar, such as RESCO, θ is equal to 180º. Hence, we will find that coherent backscattered echoes will be received by the RESCO radar when 3-meter plasma irregularities are present in the electrojet. Besides indicating the presence of these irregularities, backscattered echoes carry information about the Doppler effect caused by the westward drift of these instabilities. Figure 1 illustrates how the Doppler frequencies are obtained from one single echo, using the RESCO acquisition system.

According to this illustration, backscattered echoes received by the antenna array are split into two identical signals. These signals are compared with the reference signals through two-phase coherent detectors which provide in-phase and quadrature signals containing the Doppler deviation in the radar frequency. Each mixed signal passes through individual 50 kHz low-pass filters in order to remove the high frequency components. The two resulting signals are the real and the imaginary component of the Doppler effect. The two components of the complex signal are sampled in time, which also corresponds to sample in height provided that the electromagnetic wave travels at the light speed. These are called range gate samples. The on-line process finished with these samples is stored in a binary file. This data processing repeats for each transmitted pulse. After 1024 pulses the binary file is closed and another file is initiated until the system is tuned off. Usually, a binary file corresponds to 6 s of radar operation, and the radar is frequently operated from 0800 to 1900 LT.

Data Analysis begins with an off-line FFT analysis. 1024-sample sets from the same range gate are processed individually. Each FFT

---

[1]   See, for example Matsushita (1951), Cohen and others authors (1962), Fejer and Kelley (1960), Fejer (1996) and many other authors.
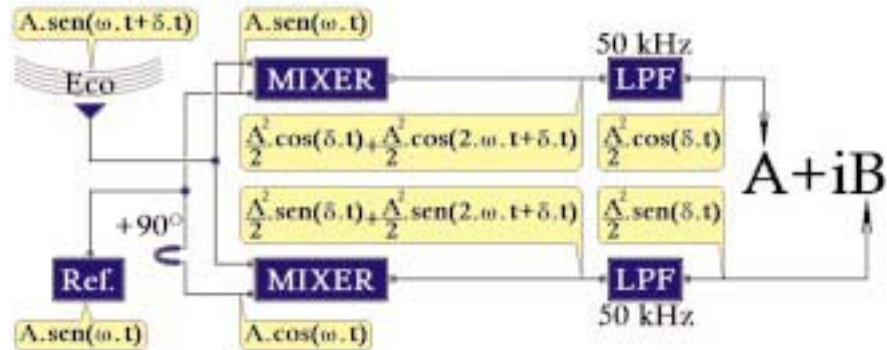
Figure 1 — Illustration of the real time data processing to obtain the Doppler effect from a single echo, which was backscatter by the 3-meter plasma irregularities and received at the RESCO radar antenna array.

Figura 1 — Ilustração do processamento de dados em tempo real para se obter o efeito Doppler de um único eco, o qual foi retroespalhando por irregularidades de plasma de três metros e coletado nas antenas do radar RESCO.

processing provides one spectral distribution of the Doppler frequencies for a given range gate (height). After analyzing all sets of 1024 samples from one range gate in each binary file acquired we have a time series of spectra. Repeating this procedure for all samples we will have several time series of spectra, each one corresponding to one range gate sounded by the RESCO radar. These series of spectra are plotted as contour color maps called spectrograms, where the x-axis corresponds to time, the y-axis corresponds to the Doppler frequency and the color scale gives the amplitude of the Fourier component. By integrating in frequency each spectrogram we are able to obtain the time variation of echo power received at the height in which the spectrogram corresponds. Now, daily Range Time Intensity (RTI) map can be obtained by grouping the time variation of echo power received per height and time. Thus, RTI maps are contour color maps with the x-axis corresponding to time, the y-axis corresponding to the height where the echo where sampled and the color scale giving the amplitude of the echo power.

RESULTS AND DISCUSSION

In December 1999 RESCO coherent backscatter VHF radar has been operated in an equatorial electrojet campaign during daytime using the switching beam operational mode. We have stored echoes from the EEJ during several days, from which we selected six representative days: three disturbed days (December 11, 12 and 13) and others three considered calm days (December 15, 16 and 17). Notice that the transition from disturbed to calm period occurred in one week only.

In this section we summarize and discuss the results we obtained during the 1999 Campaign. In figure 2 we present the three disturbed days. For each day, the top panel shows 1-minute resolution auroral indices AL (red line) and AU (blue line) referred to the left scale, and the hourly ring current index D_{st} (green line) referred to the right scale. The bottom panel shows the daily RTI map superimposed to the magnetic field H-component variation (that is, the ΔH variation with respect to the midnight values of the H-component) over two sites: Jicamarca (12° S, 76.9° W, dip: 1°) in Peru, and Vassouras (22.4° S, 43.7° W, dip: -34°) in Brazil. The bottom panel also shows the disturbed effect obtained from the difference between Jicamarca and Vassouras H-component variation.

The auroral indices of the three disturbed days are marked by several episodes of intensification and decay that are characteristics of sub-storms, while the D_{st} increase that characterizes a magnetic storm event occurred only on December 13. On December 12 we emphasize the three sub-storms: at 1300 UT (morning local time), at 1500 UT (around local midday), and at 1915 UT (later in the local noon). During the first one we see no correlation between the auroral indices and the disturbed effect; nevertheless, we certainly see correlation between the auroral indices and the backscattered power from the EEJ irregularities. In the evening no correlation is observed either with the RTI map.
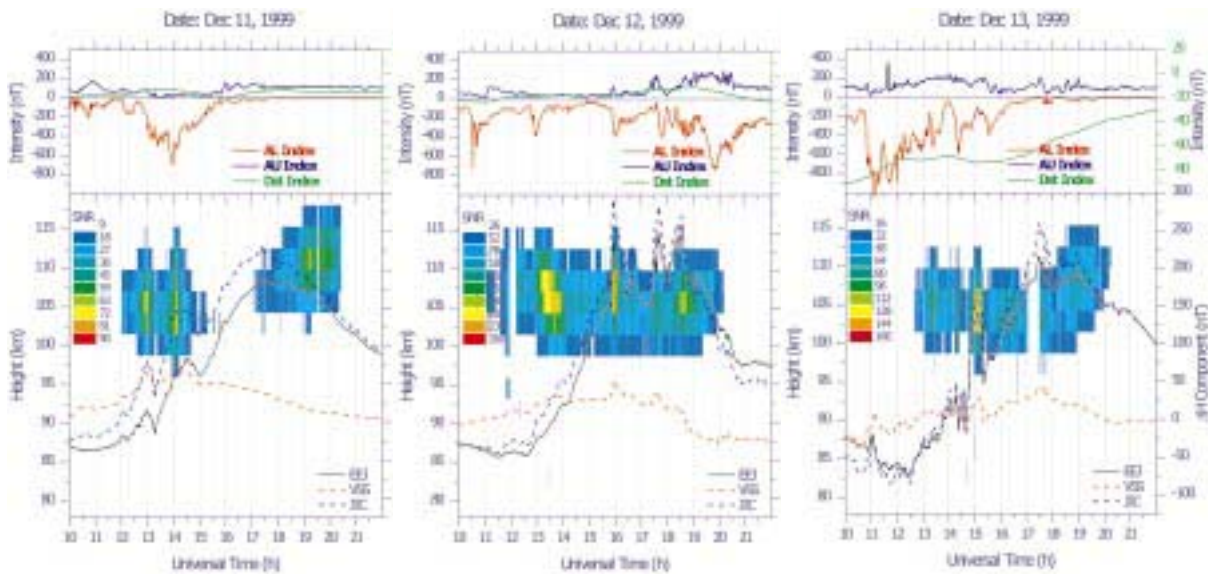
Figure 2 – Range Time Intensity (RTI) maps from three disturbed days: December 11th, 12th and 13th. The top panel of each graph shows the auroral indices (AU and AL) and the ring current index (Dst). The bottom panel shows the RTI map superimposed by the horizontal component of the Earth magnetic field measured with magnetometer at Vassouras (red dashed curve) and Jicamarca (blue dashed curve).

The black line also superimposed to the RTI map is the EEJ estimated effect.

Figura 2 – Mapa de variação temporal de intensidade (RTI) dos três dias perturbados: 11, 12 e 13 de dezembro. O gráfico superior de cada figura mostra a variação dos índices aurorais (AU e AL) e do índice da corrente anelar (Dst). Os gráficos inferiores mostram o mapa RTI sobreposto pela componente horizontal do campo magnético terrestre medido com magnetômetros em Vassouras (linha vermelha tracejada) e Jicamarca (linha azul tracejada). A linha preta, também sobreposta ao mapa RTI, é o efeito perturbado estimado.

However, around midday we observe an excellent correlation among the auroral indices, the disturbed effect, and backscattered power. The characteristics of these correlations during this day can be explained by the variation of the ionospheric conductivity throughout the day. Earlier in the morning and latter in the noon the ionospheric conductivity is very low compared with that around midday, when the ionization rate is very high. This low conductivity in these periods strongly decreases or totally inhibits the effects of field propagations and, in some cases.

On December 13 a strong magnetic storm (-1000 nT) starts at 1045 UT and continues until almost 1400 UT. It seems also that two other storms start during its recovery phase. The variation in the auroral indices and disturbance *H*-component during 1000-1700 UT on December 13 are shown blown out in figure 3 for more detailed examination of the correlation between these two parameters. In the upper panel of this figure the daily variation of 1-minute auroral index on December 13 is superimposed to that of December 14, a very quiet day. In the lower panel of this figure the disturbance *H*-component

variation on December 13 over Jicamarca is compared with that of December 14 taken as a reference quiet day curve. These curves may not represent the absolute values of the *H*-component variation over Jicamarca due to the use of Vassouras data to generate these difference curves as explained before. But the longitude separation between these two stations is small enough to yield the correct magnitude of the disturbed EEJ current fluctuations for this longitude sector as has been shown by Abdu et al. (2003).

In this figure we can see that the first, second, and third storms start around 1045 UT, 1400 UT and 1515 UT, respectively as marked by the vertical dashed lines. The second vertical dashed line marks the beginning of the recovery phase of the first storm. The main points of the comparison between the AE and the ΔH variation can be noted as follows: (a) an initial increase in ΔH that occurred around 1100 UT (0800 LT) seems to be produced by an eastward PP electric filed caused by the rapid increase of AE as was the case during the events of the previous days (GONZALES et al., 1979; SASTRI; RAO; RAMESH, 1993;
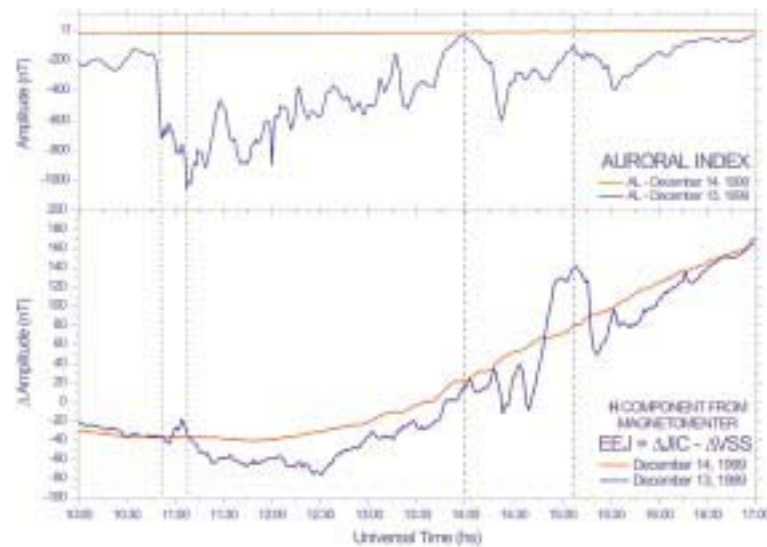
Figure 3 – Evolution of the sequence of storms (top panel) seen in the auroral index, which happened on December 13th, 1999 (blue line), related with magnetometer data (bottom panel). And the auroral index and the magnetometer data for December 14th, 1999 (red line), which is a very quiet day.
Figura 3 – Evolução da seqüência de tempestades (gráfico superior) vista no índice auroral, a qual ocorreu dia 13 de dezembro de 1999 (linha azul), relacionada com dados de magnetômetros (gráfico inferior). A linha vermelha mostra a variação do índice auroral e os dados de magnetômetros de 14 de dezembro de 1999, que foi um dia magneticamente calmo.

ABDU et al., 1997; ABDU et al., 1998); (b) the subsequent depletion observed in ΔH seams to be caused by a westward electric filed caused by the disturbance dynamo (MAZAUDIER; VENKATESWARAN, 1990); and (c) during the other two events of AE intensification, starting near 1400 UT and 1500 UT, the ΔH responds with an opposite/ambiguous phase relationship. This latter point and the related aspect of the 3-meter irregularity generation discussed above appear to be important questions to be recognized in the study of EEJ response to PP electric fields associated with AE activity. When the second storm (-600 nT) starts, its effect in the EEJ is not clear. It seems that an oscillation in the electric field begins and is amplified when the third storm (-400 nT) is triggered. Somehow, despite the second storm intensity being lower than the first, its disturbance effect is more pronounced than the first one, with respect to the amplitude variation during the disturbed period. The same happens with the third storm in comparison with the second one indicating that a superposition effect may be taking place.

On December 11 (left graph of figure 2) an AE intensification (of $\sim$200 nT) had onset at 1200 UT (0900 LT) which coincided with a minor increase in the 3-meter echo at the start of the RTI map on this day. The event that had duration of $\sim$4 hours was structured by series of short-lived enhancements and decay phases. We identify the more noticeable ones around 1200, 1300, 1400 and 1430 UT which are associated with corresponding structures in the H-component and the 3-meter echo power. The AE increases of relatively larger amplitudes (1300 and 1400 UT) produce correspondingly larger amplitudes of H increases and 3-meter irregularity power as compared the relatively weaker AE increases (1200 and 1430 UT) that produced much weaker effects in both. It may be noted further that the larger AE increases are also associated with significant broadening of the irregularity echo region. It may be verified further that the decreasing phase of the AE indices that followed each of these increases produced corresponding decrease in the H-component and 3-meter echo power. This behavior suggests that AE increases (decreases) in these cases were associated with prompt penetration disturbance electric fields (PP electric fields of eastward (westward) polarity that caused generation (decay) of 3-meter irregularities and enhancement (decay) in H-component. With respect to the complete disappearance of the EEJ echoes after midday, we need the measurements of thermospheric winds at the EEJ altitudes to confirm that the neutral atmosphere itself caused it. But the absence of perturbations in the horizontal component of the magnetic field gives

us a strong indication that the disappearance could be caused by the neutral atmosphere.

Figure 4 shows the three selected days from the disturbed period. The arrangement of the panel and the variables presented are the same as that of the three selected days from quiet period in figure 2. In these graphs we see a very poor correlation between the auroral activity and the magnetometer data or echoes from the EEJ, except at some isolated times. In December 15 we emphasize some correlation between the horizontal component of the magnetic field and the echoes from the EEJ at 1530, 1645 and 1815 UT. In December 16 this correlation occurs at 1300, 1515 and 1645 UT, and in December 17 there are correlations at 1335 and 1445 UT. But during all these days the auroral index remained extremely quiet, except early in the morning on December 17.

These RTI maps illustrate the day-to-day variability in the EEJ format and intensity. We observe that there is no repetition in the time when the maximum power scattering is observed. The event occurred after midday on December 15, before midday on December 16 and spread around midday on December 17. The main difference between the RTI patterns of the disturbed days and those of the quiet days is that in the latter case they are characterized by larger echo power with relatively more continuous patterns in contrast with the weaker power and transient patches related to the AE fluctuations in the former case. There are significant fluctuations in the RTI pattern in the latter case whose cause needs to be sought in local neutral dynamics peculiar to the observing site. For example, on December 15 the 3-meter echo power is totally absent until around midday (1500 UT) over São Luís even when the magnetic activity is very quiet. It may be noted that the H variation over Jicamarca shows lower than normal intensity during this period. Thus the generally weak electrojet in Brazil and Peru might suggest the role of neutral wind patterns in an extended geographic region. The role of such neutral dynamics is evident in the modulation of RTI pattern observed also on the other two days as well. A clear rise in the height of maximum echo power is observed in the afternoon of December 15, and to a lesser degree on the 16th. This aspect is being investigated further. Although considered a quiet day in this work, the December 17 does present some minor AE disturbances whose effect on 3-meter irregularities and ΔH have largest amplitudes near midday in agreement with such results discussed before.

Figure 5 shows three graph composed by five spectrograms each one from the disturbed period: December 11, 12 and 13, while figure 6
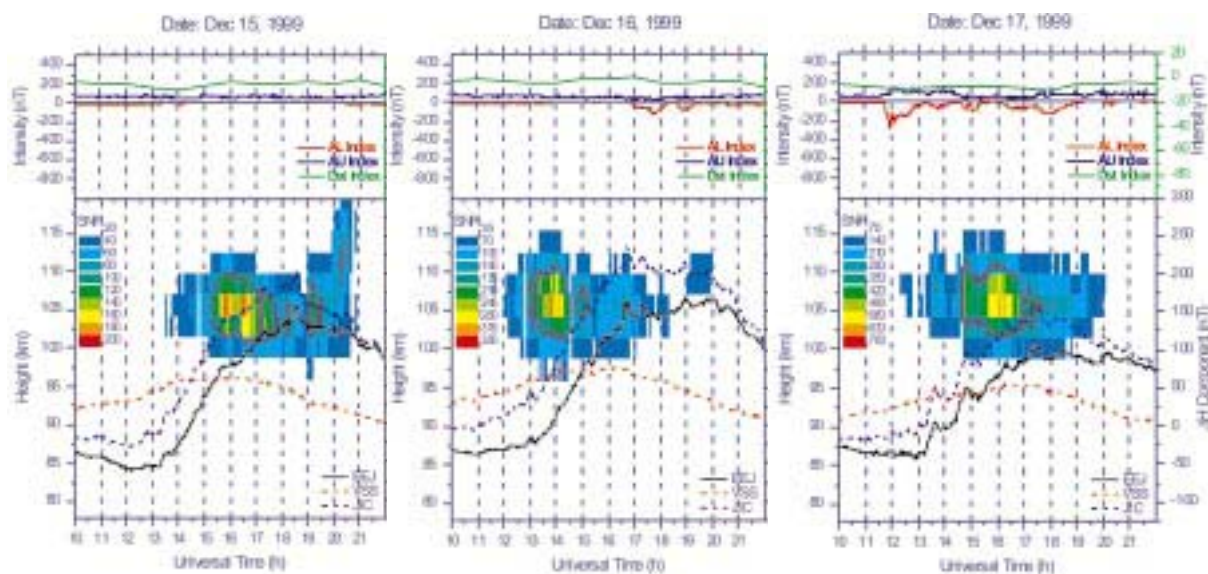

Figure 4 — Range Time Intensity (RTI) maps from three quiet days: December 15th, 16th and 17th. The top panel of each graph shows the auroral indices (AU and AL) and the ring current index (Dst). The bottom panel shows the RTI map superimposed by the horizontal component of the Earth magnetic field measured with magnetometer at Vassouras (red dashed curve) and Jicamarca (blue dashed curve). The black line also superimposed to the RTI map is the EEJ estimated effect.
Figura 4 — Mapa de variação temporal de intensidade (RTI) dos três dias calmos: 15, 16 e 17 de dezembro. O gráfico superior de cada figura mostra a variação dos índices aurorais (AU e AL) e do índice da corrente anelar (Dst). Os gráficos inferiores mostram o mapa RTI sobreposto pela componente horizontal do campo magnético terrestre medido com magnetômetros em Vassouras (linha vermelha tracejada) e Jicamarca (linha azul tracejada). A linha preta, também sobreposta ao mapa RTI, é o efeito perturbado estimado.

shows other three similar graphs from the calm period: December 15, 16 and 17. Each daily spectrogram is the set of all one-minute averaged Doppler spectra calculated for the corresponding range gate as explained in the previous section. Each one cover 2.6-km height ranging from 98.7 to 111.7 km. The height indicated in the left bottom corner of each graph corresponds to the center height of the range gate where the spectrogram was obtained.

In this set of graphs it is possible to identify three distinct regions. There is an upper region where almost only Farley-Buneman instabilities are observed and a lower region where there is great predominance of Gradient Drift instabilities. And also, there is like an intersection region
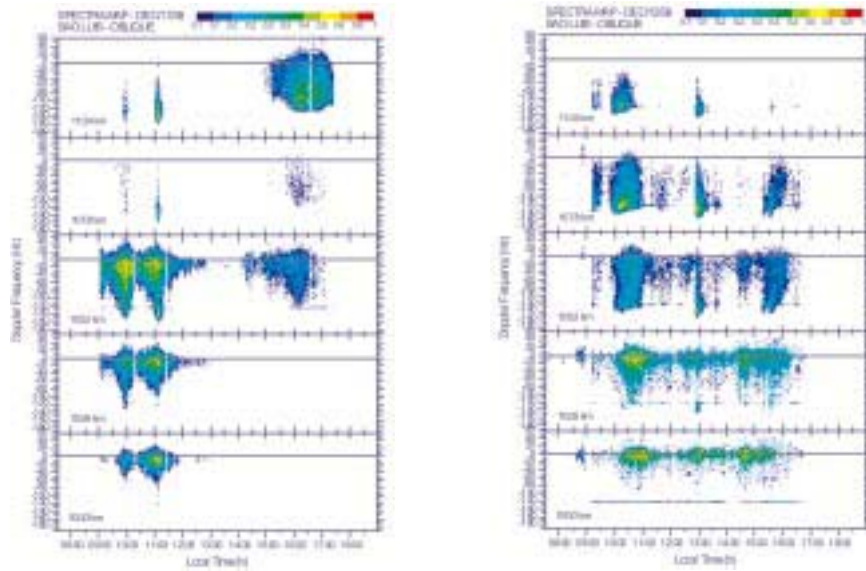

Figure 5 — Set of spectrograms from three disturbed days: December 11th, 12th and 13th, corresponding to the RTI maps from Figure 2.
Figura 5 — Conjunto de espectrogramas para os três dias perturbados: 11, 12 e 13 de dezembro, correspondentes aos mapas RTI da Figura 2.
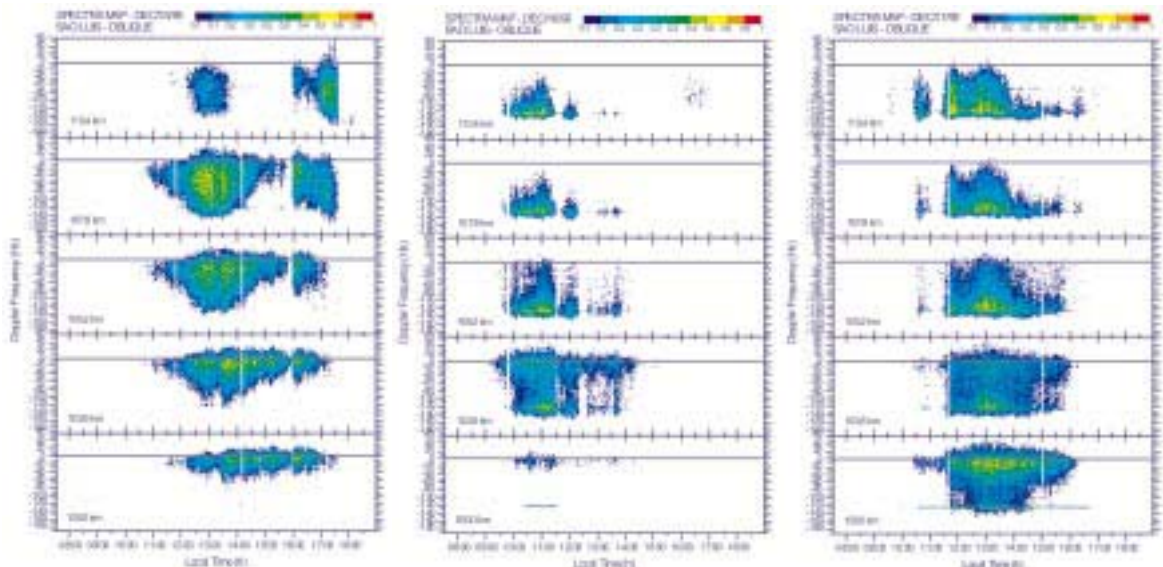

Figure 6 — Set of spectrograms from three calm days: December 15th, 16th and 17th, corresponding to the RTI maps from Figure 4.
Figura 6 — Conjunto de espectrogramas para os três dias calmos: 15, 16 e 17 de dezembro, correspondentes aos mapas RTI da Figura 4.

where both type of irregularities were observed. However, there is an interesting difference in the limits of the lower region during disturbed and calm periods.

During quiet time the lower region was observed below about 100 km. The intermediate region was observed between about 102 - 105 km, and the higher region was observed over about 110 km, despite the marked day-to-day variations. During the disturbed time the three distinct regions were also observed but Gradient Drift instability echoes extended to quite higher altitudes, depending on the disturbance conditions. The lower region was observed below about 100 - 102 km, whereas the intermediate region was observed between about 102 - 108 km, and the higher region was observed over about 110 km.

On December 13, there is also a lowering in the Farley-Buneman instability velocities after around 1500 UT. In fact, this apparent effect is not real. The rising in the EEJ irregularities seen in the RTI map is responsible for it. This rising observed in the EEJ in the Brazilian sector as well as the lowering in the instability velocities is discussed in the paper from Abdu and others (2002).

CONCLUSIONS

This work intends to demonstrate the diversity of phenomena in the EEJ and their variability in the Brazilian sector. Indeed, a quantitative work is in progress and some aspects discussed here can be better verified. However, the present work gives us a good indication of some important aspects of the EEJ during quiet and disturbed conditions from a 1-week campaign data.

During quiet conditions: (1) large degree of variability of the EEJ current strength and irregularity power are observed over São Luís even under 'quiet' conditions during the period of this study; (2) there are marked day-to-day variations; and (3) there is poor correlation between the ΔH and the EEJ backscattered power and the agreements are believed to be due to the EEJ itself. The characteristics of the variability of the EEJ current strength would suggest the role of neutral winds over extended geographic area in the South American sector. The lack of data on the neutral winds does not however permit a confirmation of this possibility on a quantitative basis.

For disturbed conditions: (1) during periods of sub-storm like auroral electrojet intensification the transient changes in the EEJ are clearly correlated with the variations in the AE indices; (2) at noon (morning / evening) hours the modulations effect are more (less) pronounced due to the high (low) ionospheric conductivity; (3) isolated event preceded by quiet conditions seems to produce more clear responses; (4) when two or more events occur in sequence the effects in

the EEJ seem to be superimposed and the analysis become more complicated; and (5) clear modulation of the EEJ becomes more evident when the auroral index AL reaches values under -400 nT. Intensification in the AE produces, in general, an enhancement in the EEJ current intensity and 3-meter plasma instabilities, which can be attributed to the prompt penetration to equatorial latitude of magnetospheric disturbance electric field of eastward polarity. The recovery phase of the AE intensification was seen to be associated with a decrease of the EEJ effects due to a PP electric field of westward polarity.

The spectral analysis of the EEJ back-scattered radar signal revealed differences in the height distributions of the Farley-Buneman and Gradient Drift plasma irregularities. We could define three distinct regions: (1) a lower region of predominance of Gradient Drift irregularities; (2) an upper region of predominance of Farley-Buneman irregularities; and (3) and intermediate region where both spectral signatures could be equally identified. We also observed differences in height of Gradient Drift scattering regions between quiet and disturbed conditions. During quiet days the lower (Gradient Drift) region was observed below about 100 km; the intermediate region (where both types of irregularities could be found) between 102 and 105 km, and the higher (Farley-Buneman) region was observed over about 110 km. During disturbed days echoes with the Gradient Drift irregularities signatures tended to be observed at higher altitudes, depending on the disturbance conditions. The lower region was observed below about 100 - 102 km. The intermediate region was observed about 102 - 108 km, and the higher region was observed over about 110 km.

REFERENCES

ABDU, M. A. et al. Equatorial disturbance dynamo electric field longitudinal structure and spread F: a case study from GUARA/EITS campaigns. *Geophysical Research Letters*, Washington DC, v. 24, n. 13, p. 1707-1710, 1997.

_____ et al. DP 2 electric field fluctuations in the dusk-time dip equatorial ionosphere. *Geophysical Research Letters*, Washington DC, v. 25, n. 9, p. 1511-1514, 1998.

_____ et al. Equatorial electrojet irregularities investigations of using a 50 MHz backscatter radar and a digisonde at São Luís: some initial results. *Journal of Atmospheric and Solar-Terrestrial Physics*, Amsterdam, v. 64, n. 12-14, p. 1425-1434, 2002.

_____ et al. Equatorial electrojet 3-m irregularity dynamics during magnetic disturbances over Brazil: results from the new VHF radar at São Luís. *Journal of Atmospheric and Solar-Terrestrial Physics*, Amsterdam, v. 65, n. 14-15, p. 1293-1308, 2003.

BALSLEY, B. B. Evidence of the nighttime current reversal in the equatorial electrojet. *Annales de Geophysical,* Toulouse, v. 22, p. 406-470, 1966. fasc. 3

COHEN, R.; BOWLES, K. L.; CALVERT, W. On the nature of equatorial slant sporadic E. *Journal of Geophysical Research,* Washington, DC, v. 67, n. A3, p. 965-972, 1962.

FEJER, B. G. Natural ionospheric plasma waves. In: KOHL, H.; RÜSTER, R.; SCHLEGER, K. (Ed.). *Modern ionospheric science,* Max–Plank Institute for Aeronomy, Katlenburg-Lindau: Germany. Cap. 8, p. 216-273.1996

_____; KELLEY, M. C. Ionospheric irregularities. *Reviews of Geophysics and Space Physics,* Washington, DC, v. 18, n. 2, p. 401-454, 1980.

FORBES, J. M. The equatorial electrojet. *Reviews of Geophysics and Space Physics,* Washington, DC, v. 19, n. 3, p. 469-504, 1981.

GONZALES, S. A. et al. Equatorial electric fields during magnetically disturbed conditions 2. Implications of simultaneous auroral and equatorial measurements. *Journal of Geophysics Research,* Washington, DC, v. 84, n. A10, p. 5803-5812, 1979

KUDEKI, E. et al. The condor equatorial electrojet campaign: radar results. *Journal of Geophysical Research,* Washington, DC, v. 92, n. A12, p. 13561-13577, 1987.

MAZAUDIER, C.; VENKATESWARAN, S. V. Delayed ionospheric effects of the geomagnetic storm of march 22, 1979 studied by the sixth coordinated data analysis workshop (CDAW-6). *Annales Geophysicae,* Toulouse, v. 8, p. 511-518, 1990.

MATSUSHITA, S. Intense E_s ionization near the magnetic equator. *Journal of Geomagnetism and Geoelectricity,* Washington, DC, v. 3, p. 44, 1951.

PFAFF, R. F. et al. *Electric field and plasma density measurements in the strongly driven daytime equatorial electroje: 1.* The unstable layer and the gradient drift waves. *Journal of Geophysical Research,* Washington DC, v. 92, n. A12, p. 13578-13596, 1987.

REDDY, C. A. The equatorial electrojet: a review of the ionospheric and geomagnetic aspects. *Journal of Atmospheric and Terrestrial Physics,* Amsterdam, v. 43, n. 5/6, p. 557-571, 1981.

_____. The equatorial electrojet. *Pure and Applied Geophysics,* Berlin, v. 131, n. 3, p. 486-508, 1989.

SASTRI, J. H.; RAO, J. V. S. V.; RAMESH, K. B. Penetration of polar electric field to the nightside dip equator at times of geomagnetic sudden commencements. *Journal of Geophysics Research,* Washington DC, v. 98, n. A10, p. 17517-17523, 1993.

NOTES ABOUT THE AUTHORS

Clezio Marcos De Nardin é formado em Engenharia Elétrica pela Universidade Federal de Santa Maria em 1997, Mestre em Geofísica Espacial pelo Instituto Nacional de Pesquisas Espaciais em 1999, e Doutor em 2003, também em geofísica Espacial pelo Instituto Nacional de Pesquisas Espaciais. Tem trabalhado com pesquisas na área de aeronomia desde sua iniciação científica, quando participou da cooperação entre o Instituto Nacional de Pesquisas Espaciais, o Laboratório Philips da força Aérea Norte-Americana e a Universidade Federal de Santa Maria (INPE / AFPL / UFSM) para estudos da Camada E_s-Esporádica e de rastros de meteoros utilizando rádio enlace em VHF. Nesta época recebeu prêmio da Associação Brasileira de Ensino de Engenharia pelo seu trabalho apresentado no XI Congresso Regional de Iniciação Científica e Tecnológica em Engenharia. Em seu mestrado, participou no desenvolvimento de um dos módulos do radar de espalhamento coerente de 50 MHz de São Luís do Maranhão (RESCO) e analisou os primeiros dados de espalhamento coerente deste radar. Em seu doutorado desenvolveu algoritmos de análise de espectros de potência característicos de irregularidade de plasma do eletrojato equatorial e calculou os primeiros valores de campos elétricos da região E Ionosférica brasileira usando esta técnica no Brasil. Tem participado de cooperações internacionais com os pesquisadores do Rádio Observatório de Jicamarca, Peru. Atualmente, é Pesquisador Adjunto do INPE e membro da equipe de pesquisadores e engenheiros do grupo da ionosfera que participam do projeto do radar RESCO.

Mangalathayil Ali Abdu é formado em Física pela Universidade de *Kerala*, Índia em 1959. Mestre em Eletrônica e Física (1961) pela Universidade de *Kerala*. Doutor Ph.D (1967), em Aeronomia pela Universidade de *Gujarat*, Índia. A pesquisa de doutorado foi desenvolvida no Departamento de Ciências Espaciais do "*Physical Research Laboratory*", *Ahmedabad*, hoje um dos centros de pesquisa e desenvolvimento do ISRO (*Indian Space Research Organization*). A sua tese de doutorado voltou-se ao estudo da ionosfera tropical e baseou-se em técnicas de absorção de sinais cósmicos pela ionosfera. Realizou pós-doutorado no Departamento de Física da Universidade de *Western Ontario*, Canadá, onde foi responsável pelo desenvolvimento de técnica de estudos ionosféricos através de traços meteóricos. Possui mais de 150 trabalhos publicados em revistas especializadas, e orientou diversas teses de mestrado e doutorado no curso de pós-graduação em Geofísica Espacial do INPE. Foi responsável pelos projetos de colaboração internacionais patrocinados pela IAGA (*International Association of Geomagnetism and Aeronomy*) e SCOSTEP (*Scientific Committee on Solar–Terrestrial Physics*). É assessor da FAPESP, do CNPq, de NSF e da NASA. Já participou do quadro de editores de revistas internacionais. Atualmente é pesquisador titular do INPE e dedica-se ao estudo da dinâmica do sistema ionosfera-termosfera-magnetosfera-meio interplanetário por meio de técnicas ópticas e de radiofreqüência.

José Humberto Andrade Sobral é formado em Engenharia Eletrônica pela Escola Nacional de Engenharia do Rio de Janeiro (atual UFRJ), em 1966, Mestre em Ciências Espaciais em 1969 pelo INPE. Doutor (Ph. D.) em 1973, pelo Departamento de Engenharia Elétrica da Universidade de Cornell (EEUU). A sua tese de doutorado foi desenvolvida no Observatório de Arecibo, em Porto Rico (*National Astronomy and Ionosphere Center/Cornell University*) com enfoque nos estudos da dinâmica da ionosfera por meio de técnicas ópticas e por radar de espalhamento incoerente. Foi admitido no INPE como pesquisador (1967). Possui mais de 90 artigos científicos em revistas especializadas internacionais e orientou diversas teses de mestrado e doutorado no curso de Pós-Graduação de Geofísica Espacial do INPE. É assessor da FAPESP, do CNPq e da NASA. Já participou do quadro de editores de revistas internacionais. Recebeu em 1987 o prêmio "MARC" da Universidade de Porto Rico/ *National Science Foundation* pelo seu trabalho de pesquisa no Observatório de Arecibo. Atualmente é Pesquisador Titular do INPE dedica-se ao estudo da dinâmica do sistema ionosfera-termosfera-magnetosfera-meio interplanetário por meio de técnicas ópticas e de radiofreqüência.